sustainability

MDPI

Article

Evaluation of the Incorporation of Tire-Derived Aggregates (TDA) in Rigid Pavement Mix Designs

Ahmad M. Abu Abdo [1,*] and Hany El Naggar [2,*]

[1] Department of Civil Engineering, Liwa College of Technology, Abu Dhabi 51133, United Arab Emirates
[2] Department of Civil & Resource Engineering, Dalhousie University, Halifax, NS B3H 4R2, Canada
* Correspondence: ahmed.abuabdo@ect.ac.ae (A.M.A.A.); hany.elnaggar@dal.ca (H.E.N.)

Abstract: Owing to the extensive worldwide generation of solid wastes, such as rubber tires, and the resulting adverse environmental impacts, the incorporation of these waste materials in construction projects has become a widespread aim. However, concerns have arisen regarding the effects of rubber waste on the mechanical properties of Portland cement concrete (PCC) mixes. Thus, this study investigates the effects of replacing natural coarse aggregates with tire-derived aggregates (TDA). In PCC mixes, natural aggregates were replaced by 0, 10, 20, 40, 60, 80, and 100% TDA by volume, and the properties of these specimens were tested in the laboratory. The results obtained were then used as inputs for the KENPAVE software, to evaluate induced stresses, deflections, and cracking indices in rigid pavement slabs, with eleven different thicknesses, ranging from 200 to 300 mm in 10 mm increments. Stresses under different loading conditions decreased as PCC slab thickness and TDA content increased. Increased deflection and cracking indices resulting from adding TDA could be counteracted by increasing the PCC slab thickness by 10 mm. Moreover, environmental impacts and cost analyses were examined via PaLATE 2.0, which showed that the use of TDA could reduce energy consumption, harmful emissions, and material costs. Overall, this study indicates that the use of TDA in PCC mixes has benefits that can make it a good candidate for sustainable, ecofriendly rigid pavement construction projects.

Keywords: rigid pavements; Portland cement concrete mixes; tire-derived aggregates; stresses; deflection; cracking index; environmental impacts; cost analyses

check for updates

Citation: Abu Abdo, A.M.; El Naggar, H. Evaluation of the Incorporation of Tire-Derived Aggregates (TDA) in Rigid Pavement Mix Designs. *Sustainability* **2022**, *14*, 11775. https://doi.org/10.3390/su141811775

Academic Editors: Ahmed R. Suleiman and Ahmed Soliman

Received: 14 June 2022
Accepted: 14 September 2022
Published: 19 September 2022

1. Introduction

There is no doubt that widespread global and regional development and urbanization are negatively affecting the environment and increasing the rate of depletion of natural resources. Industries related to development and processing not only accelerate climate change and global warming due to their large carbon footprint, but also generate an enormous amount of solid waste. Solid wastes typically include organics, paper, glass, plastics, metals, wood, rubber tires, etc. Their disposal generally involves dumping in landfills or incineration for energy production, which may result in severe environmental problems, including air quality degradation, water pollution, and the utilization of valuable land areas. However, if properly treated and processed, solid waste can become a sustainable source of useful construction materials. Portland cement concrete (PCC) mixes are a primary component of construction projects worldwide. Owing to the depletion of raw materials used in PCC mixes (e.g., rocks, water, limestone, shells, chalk, marl, and other materials) as a result of recent development and urbanization, together with the negative environmental impacts associated with the manufacturing processes, the private sector and public agencies are currently focused on finding sustainable green alternative materials, such as, cellulosic spinney waste fibers [1], bitumen as a cement–bitumen composite [2], glass waste [3], polymers [4], nanomaterials [5], polyvinylchloride (PVC) pipes and asphaltene [6], and plastic waste [7].

Tire-derived aggregate (TDA) is a relatively new construction material, produced by shredding scrap tires into small pieces ranging in size from 12 mm to 305 mm. TDA has useful properties, maintains its structural integrity, and weighs 70% less than conventional gravel. TDA has been used for decades as a lightweight construction material in various civil engineering applications, such as road construction, and deployment under foundations, and around buried utilities [8–21].

Portland cement concrete (PCC) mixes are a primary component of construction projects worldwide. Owing to the depletion of raw materials used in PCC mixes (e.g., crushed rocks, limestone, chalk, marl, and other materials) resulting from the recent expansion of development and urbanization as well as the negative environmental impacts associated with manufacturing processes, the search for alternative construction materials for greener, more sustainable solutions has intensified.

Researchers have been investigating the utilization of different types of waste in concrete, to enhance its properties and improve its functionality. The waste materials evaluated include recycled construction materials, plastic waste, glass, rubber tire waste, and steel manufacturing byproducts [21–26]. Molenaar [27] has suggested that the utilization of recycled and waste materials in road construction projects could reduce their carbon footprint while generating economic and environmental benefits.

Cement-based concrete is a brittle material with high rigidity and relatively poor damping properties. Some applications, such as pavement and traffic barriers, require concrete with greater toughness and impact resistance. The use of rubberized concrete has therefore been gaining acceptance in the past decade as a means of increasing the deformability and ductility of concrete [20].

Many studies have been conducted to examine the implications of adding TDA to PCC mixes. Findings have shown that increased rubber content has a negative effect on preferred PCC mechanical properties but improves ductility and material toughness [28]. Bandarage and Sadeghian [11] have reported that the replacement of fine materials with shredded rubber particles resulted in failure patterns differing from those of a typical PCC mix. On the other hand, some studies have indicated that PCC mixes containing rubber could be incorporated in concrete structural elements, providing sufficient strength and adequate service life [29,30], with the added benefit of permitting the absorption of a large amount of plastic energy under different loading conditions [8,19].

2. Objectives

The main objective of this study was to investigate how the replacement of natural coarse aggregates with different percentages of tire-derived aggregate (TDA) affects the performance of PCC pavements. In addition, the study evaluated the cost savings and environmental impacts resulting from incorporating TDA in rigid pavement construction.

3. Experimental Program

3.1. Materials

The specimens used in this research were fabricated by utilizing locally sourced materials. Recycled TDA rubber was obtained from a local scrap tire recycling plant. The TDA used was sieved in the laboratory and all TDA particles larger than 19.05 mm were removed. A sieve analysis was also conducted on the different constituents of the concrete matrix, in accordance with ASTM C136. The material properties of the concrete constituents are listed in Table 1. TDA was used to replace natural coarse aggregates in the PCC mix in six different percentages: 10, 20, 40, 60, 80, and 100% TDA by volume. For purposes of comparison, a control mix with 0% TDA was also prepared. Three cylinders 150 mm in diameter and 300 mm high and beams measuring 150 $\times$ 150 $\times$ 500 mm were made from each mix. Table 2 lists the constituents of a typical PCC mix used in this study.

Table 1. Material properties of the constituents used.

Material	Type	Minimum Aggregate Size (mm)	Maximum Aggregate Size (mm)	Bulk Density (kg/m^3)
Cement	PC Type 1	_	_	1506
Fine aggregates	Masonry sand	0.15	4.75	1817
Coarse aggregates	12 mm gravel	4.75	19.05	1601
TDA *	Shredded tires	4.75	19.05	557

* TDA aspect ratio is approximately 1:2.5.

Table 2. PCC control mix constituents.

Material	Weight, kg
Cement	569
Water	235
Fine aggregates	559
Coarse aggregates	958

3.2. Laboratory Tests

To investigate the effects of adding TDA to PCC mixes, seven concrete mixes with different TDA percentages were prepared. Mix with 0% TDA acted as the control mix. The cement content, water–cement ratio, and volume of aggregate were kept constant for all mixes. In each mix, TDA replaced a certain percentage of the natural coarse aggregate by volume. Three specimens of each type of mix were prepared to determine the average for each of the properties examined. The effect of the TDA content on the compressive strength, elastic modulus, and flexural strength of the concrete at 28 days was measured by utilizing the ASTM testing procedures ASTM C39, ASTM C469M, and ASTM C78, respectively. The results obtained were then used as inputs for the KENPAVE software, a computer package for pavement analysis and design, in order to study the effects of using TDA in concrete pavement.

3.3. KENPAVE Software

Stresses, deflections, and damage ratios (cracking index, *CI*) of rigid PCC pavements resulting from tire loading were determined via the KENPAVE software [31]. KENPAVE employs the finite element method (FEM) by constructing a rectangular finite element mesh with assigned corner nodes to represent the PCC slabs. The software modeled concentrated vertical forces at the nodes due to wheel loading, and applied subgrade reactions to the PCC slab to represent the stiffnesses of the base and subbase structures; a detailed description of KENPAVE software and its algorithms can be found in Huang [31]. Concrete slabs with eleven different thicknesses, ranging from 200 to 300 mm in 10 mm increments, were considered in order to evaluate the effects of incorporating different percentages of TDA in rigid pavements. The subgrade used under the slab had a modulus of subgrade reaction of 55 MN/m^3, representing a typical stiffness for base layers under rigid pavements. A 6000 kg dual-wheel load with 350 mm spacing and a contact pressure of 550 kPa was applied first at the corner of the slab, then at the interior of the slab, and finally at the edge of the slab (Figure 1) to determine the stresses, deflections, and damage resulting from the applied load. With the aid of Portland Cement Association (PCA) models, KENPAVE uses the PCC elastic modulus to determine stresses and deflection, and the modulus of rupture to determine the cracking index (Equations (1)–(4)). The cracking index (*CI*) can be defined as “the summation of the ratio of the number of load repetitions to the maximum allowable number of load repetitions (N_f) and is a function of the flexural strength of PCC mixes” [31]. Pavement failure occurs when *CI* reaches a value of 1. Equation (3) represents unlimited loading cycles, where *CI* = 0 (i.e., no failure occurs). This is related to the endurance limit of PCC mixes [31].

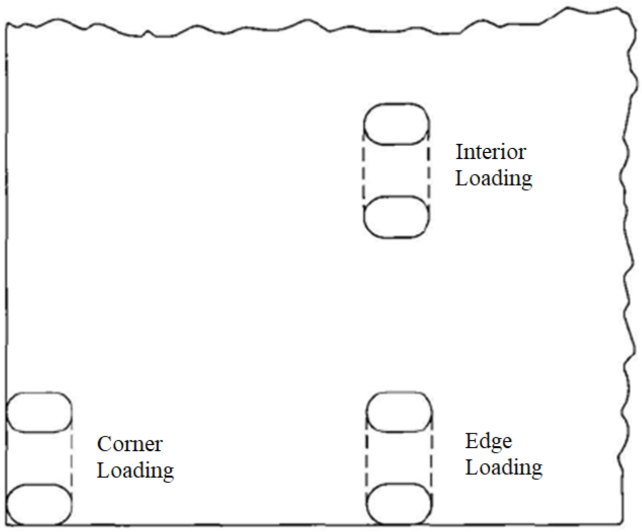

Figure 1. Types of loading condition conditions (after Huang [31]).

$$For\ \frac{\sigma}{S_c} \geq 0.55: \quad logN_f = 11.737 - 12.077\left(\frac{\sigma}{S_c}\right) \tag{1}$$

$$For\ 0.45 < \frac{\sigma}{S_c} < 0.55: \quad N_f = \left(\frac{4.2577}{\sigma/S_c - 0.4325}\right)^{3.268} \tag{2}$$

$$For\ \frac{\sigma}{S_c} \leq 0.45: \quad N_f \text{ is unlimited} \tag{3}$$

where

σ = flexural stress in the slab, MPa;
S_c = the modulus of rupture of the PCC mix, MPa.

$$CI = \sum_{i=1}^{p}\sum_{j=1}^{m}\frac{n_{i,j}}{N_{f_{i,j}}} \tag{4}$$

where

$n_{i,j}$ = the predicted number of load repetitions for load j in period i;
$N_{fi,j}$ = the allowable number of load repetitions, determined by Equations (1)–(3);
p = the number of periods per year;
m = the number of load groups.

3.4. Environmental Impacts and Cost Analyses

Vast quantities of rubber tires are manufactured annually worldwide, resulting in a massive amount of rubber tire waste. In 2017, 249.4 million scrap tires were generated in the USA alone, with 16% being disposed of in landfills or burned as an alternative source of energy. However, the burning of rubber tires leads to severe environmental impacts, including toxic air emissions, and water and soil pollution [32]. Thus, rubber tire waste can negatively affect the environment and public health and safety.

To evaluate the effects of using TDA in rigid pavements, a rigid pavement lane 1 km long and 4 m wide was considered. Eleven different slab thicknesses were used, ranging from 200 to 300 mm in 10 mm increments, together with seven different PCC mixes, where coarse material aggregates were replaced by 0, 10, 20, 40, 60, 80, and 100% TDA by volume. To facilitate comparisons between the different mix designs, only the initial construction phase was considered. The pavement lifecycle assessment tool for environmental and economic effects, PaLATE 2.0 (Madison, WI, USA), was used to evaluate the environmental impacts and initial construction material costs of the different designs. Material production, transportation, and processes and equipment used in construction were considered, together with cost analyses including materials. PaLATE 2.0 utilizes spreadsheets with design specifications, material estimates, and energy consumption specifications for construction and maintenance machinery. The PaLATE 2.0 software tracks material and energy flows, emissions, and design, construction, operation, and maintenance costs. Dos Santos et al. [33] evaluated different types of lifecycle analysis software tools, including PaLATE, GaBi, DuboCalc, and ECORCE-M. They found that although the results of the different tools varied for specific impact categories, most of the software tools were able to determine the approximate overall environmental impacts of the pavements assessed. Advantages of using PaLATE 2.0 include its ease of access and the possibility of modifying its materials and process databases, which take local conditions into account. Further details concerning PaLATE 2.0 can be found in Horvath [34] and Bloom [35]. PaLATE 2.0 evaluates the following environmental impacts:

- Energy consumption;
- Water consumption;
- Carbon dioxide (CO_2) and global warming potential (GWP);
- Nitrogen oxides (NO_x);
- Particulate matter (PM_{10});
- Sulfur dioxide (SO_2);
- Carbon monoxide (CO);
- Mercury (Hg);
- Lead (Pb);
- Resource Conservation and Recovery Act (RCRA) hazardous waste generated;
- Human toxicity potential (cancer), an index that reflects the potential harm of a unit of chemical released into the environment;
- Human toxicity potential (noncancer), accounting for adverse health effects on human beings caused by the intake of toxic substances.

4. Results and Analysis

4.1. Strength and Stiffness Properties

Figure 2 shows the 28 day compressive strength measured for the seven concrete mixes evaluated. The compressive strength of the mixes containing TDA was lower than that of the control case, which contained no TDA. For a mix where 10% of the natural coarse aggregate was replaced by TDA, a 25% strength reduction was observed, and for the mix with 100% TDA, a 79% strength reduction was seen. The causes of decreased concrete compressive strength with increasing TDA content have been explained in various studies [20,36–38]. This reduction in strength is attributed primarily to the very low stiffness of rubber compared to the other concrete constituents. The rubber thus acts as a void in the concrete matrix. In addition, the smooth surface of rubber results in low adhesion between the TDA particles and the cement paste.

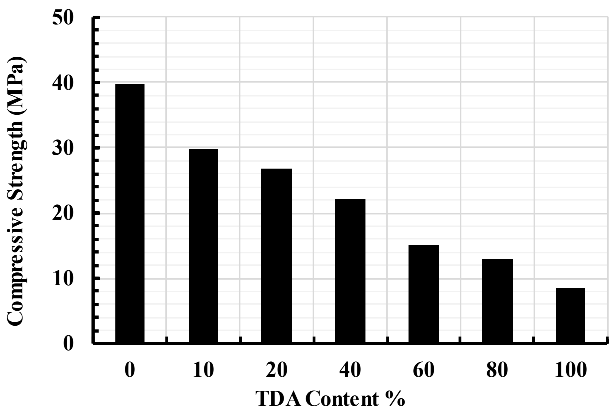

Figure 2. Variation of the compressive strength of rubberized concrete with TDA content.

Although the inclusion of rubber in concrete substantially enhances the ductility of the concrete, it reduces the modulus of elasticity, as can be seen in Figure 3. The low stiffness and soft structure of the TDA particles lead to high energy absorption and ductility before failure, which is a very desirable feature in concrete pavement applications. As shown in Figure 3, similar to the observed reduction in compressive strength, in comparison to the control case with 0% TDA, the elastic modulus decreased by approximately 36% in concrete mixes where 10% of the natural coarse aggregate was replaced by TDA, and by 84% in mixes with 100% TDA.

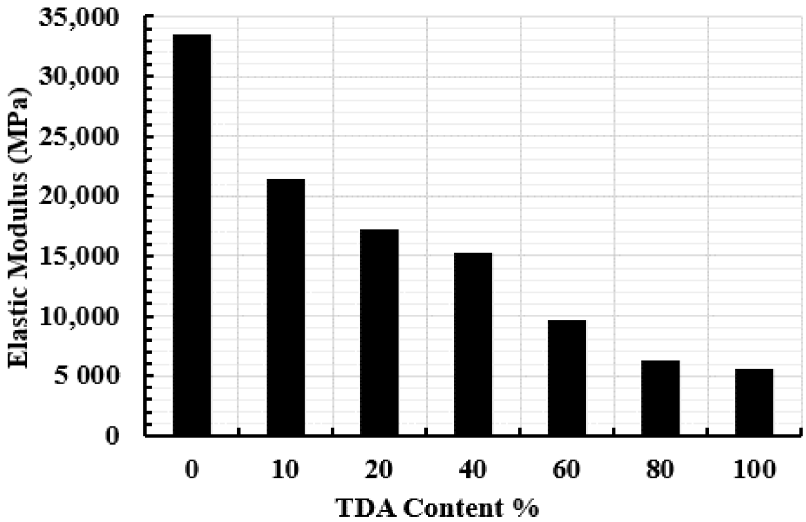

Figure 3. Variation of the elastic modulus of rubberized concrete with TDA content.

Similarly, the decrease in flexural strength of rubberized concrete seen in this study is similar to that observed for the compressive strength. Figure 4 plots the modulus of rupture against the percentage of coarse aggregate replaced by TDA. In comparison to the control mix with 0% TDA, flexural strength was reduced by 22% in mixes with 10% TDA, and by 59% in mixes with 100% TDA. However, it should be noted that an advantage of rubberized concrete is that it does not exhibit brittle failure, as conventional concrete does under bending loading conditions.

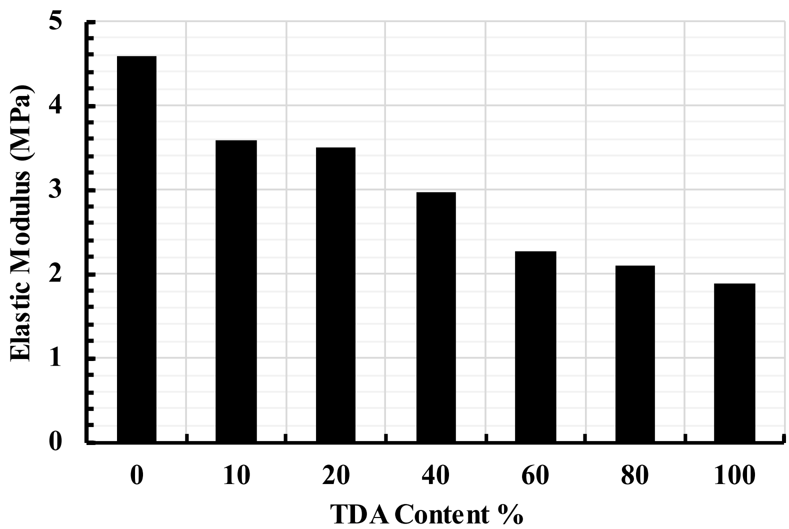

Figure 4. Variation of the modulus of rupture of rubberized concrete with TDA content.

4.2. KENPAVE Software

KENPAVE software results showed that for the evaluated PCC mixes, the stresses resulting from the three loading conditions decreased linearly with increasing TDA content, as illustrated in Tables 3–8. Figure 5 shows the maximum stresses resulting in the x- and y-directions for selected slab thicknesses. The negative values correspond to tensile stresses, whereas the positive values correspond to compressive stresses. The stresses generated decreased as the PCC slab thickness and TDA content increased. Due to the ductile, flexible nature of TDA, it seems probable that the TDA acts as a cushion and reduces the effects of the applied loads on the PCC slab, yielding lower resulting stresses in all directions.

Table 3. Stresses in slab with thickness of 200 mm.

TDA, %	**0**	**10**	**20**	**40**	**60**	**80**	**100**
Corner Loading							
Max stress, kPa	1798.8	1672.5	1603.6	1565.5	1411.2	1275.5	1236.4
Max comp. stress (x-direction), kPa	1484.4	1430.9	1395.9	1374.9	1279.4	1164.6	1129.8
Max tensile stress (x-direction), kPa	−86.9	−26.4	0	0	−2.8	−5.8	−10
Max comp. stress (y-direction), kPa	1288.9	1184.4	1124.8	1091.2	1004.7	944.9	926.6
Max tensile stress (y-direction), kPa	−725.2	−657.8	−624.4	−606.7	−540.7	−480.6	−465.1
Interior Loading							
Max stress, kPa	−1361.4	−1273.4	−1230.3	−1207.5	−1120.6	−1037.0	−1014.4
Max comp. stress (x-direction), kPa	228.2	233.4	231.4	229.1	212.9	192.2	198.2
Max tensile stress (x-direction), kPa	−1361.4	−1273.4	−1230.3	−1207.5	−1120.6	−1037.0	−1014.4
Max comp. stress (y-direction), kPa	307.5	302.8	299.3	297.0	285.9	271.6	267.1
Max tensile stress (y-direction), kPa	−397.2	−389.5	−385.6	−383.4	−374.9	−366.4	−364.1
Edge Loading							
Max stress, kPa	−2503.9	−2335.8	−2253.9	−2210.7	−2046.9	−1890.9	−1848.9
Max comp. stress (x-direction), kPa	412.9	423.4	419.6	415.3	384.7	336.7	334.3
Max tensile stress (x-direction), kPa	−2503.9	−2335.8	−2253.9	−2210.7	−2046.9	−1890.9	−1848.9
Max comp. stress (y-direction), kPa	501.5	456.9	431.4	417.0	385.7	370.9	366.2
Max tensile stress (y-direction), kPa	−294.5	−280.6	−274.0	−270.8	−258.8	−248.9	−246.5

Table 4. Stresses in slab with thickness of 220 mm.

TDA, %	**0**	**10**	**20**	**40**	**60**	**80**	**100**
Corner Loading							
Max stress, kPa	1551.5	1450.7	1398.2	1368.8	1247.9	1128.6	1097.6
Max comp. stress (x-direction), kPa	1245.8	1212.9	1190.1	1176	1109.5	1025.9	1000.1
Max tensile stress (x-direction), kPa	−102.6	−53.9	−29.1	−15.8	0	−3.7	−4.4
Max comp. stress (y-direction), kPa	1110.3	1036.2	992.5	967.4	861.1	814.1	800.6
Max tensile stress (y-direction), kPa	−633.8	−579.4	−551.8	−537	−481	−428.9	−415.3
Interior Loading							
Max stress, kPa	−1172.4	−1098.6	−1062.7	−1043.8	−971.3	−901.7	−882.8
Max comp. stress (x-direction), kPa	180.4	191.3	192.9	192.7	185.5	169.3	163.6
Max tensile stress (x-direction), kPa	−1172.4	−1098.6	−1062.7	−1043.8	−971.3	−901.7	−882.8
Max comp. stress (y-direction), kPa	255.2	253.0	251.0	249.6	242.4	232.5	229.2
Max tensile stress (y-direction), kPa	−332.0	−326.0	−322.9	−321.1	−314.3	−307.4	−305.5
Edge Loading							
Max stress, kPa	−2160.1	−2018.5	−1950.1	−1914.0	−1776.8	−1646.0	−1610.7
Max comp. stress (x-direction), kPa	325.0	346.7	349.9	349.6	336.0	305.5	294.6
Max tensile stress (x-direction), kPa	−2160.1	−2018.5	−1950.1	−1914.0	−1776.8	−1646.0	−1610.7
Max comp. stress (y-direction), kPa	433.4	402.0	383.4	372.6	327.2	314.9	311.5
Max tensile stress (y-direction), kPa	−250.9	−239.2	−233.5	−230.6	−219.9	−210.8	−208.6

Table 5. Stresses in slab with thickness of 240 mm.

TDA, %	0	10	20	40	60	80	100
Corner Loading							
Max stress, kPa	1350.2	1266.8	1226.5	1203.7	1108.4	1005.7	978.1
Max comp. stress (x-direction), kPa	1066.7	1037.0	1022.2	1012.8	966.5	905.5	886.1
Max tensile stress (x-direction), kPa	−108.5	−69.5	−49.0	−37.9	0.0	−0.8	−2.1
Max comp. stress (y-direction), kPa	961.9	909.0	876.9	858.1	776.5	706.4	696.5
Max tensile stress (y-direction), kPa	−557.4	−513.8	−491.0	−478.7	−431.1	−386.0	−374.0
Interior Loading							
Max stress, kPa	−1022.0	−959.1	−928.6	−912.5	−851.2	−792.3	−776.2
Max comp. stress (x-direction), kPa	142.2	156.5	160.3	161.5	160.4	151.1	147.3
Max tensile stress (x-direction), kPa	−1022.0	−959.1	−928.6	−912.5	−851.2	−792.3	−776.2
Max comp. stress (y-direction), kPa	214.7	213.9	212.9	212.1	207.5	200.6	198.3
Max tensile stress (y-direction), kPa	−281.6	−276.9	−274.4	−273	−267.5	−261.8	−260.2
Edge Loading							
Max stress, kPa	−1886.2	−1765.0	−1706.5	−1675.8	−1559.2	−1447.9	−1417.8
Max comp. stress (x-direction), kPa	254.8	282.8	290.4	292.7	290.9	273.4	266.2
Max tensile stress (x-direction), kPa	−1886.2	−1765	−1706.5	−1675.8	−1559.2	−1447.9	−1417.8
Max comp. stress (y-direction), kPa	376.1	354.1	340.5	332.5	297.5	269.8	267.5
Max tensile stress (y-direction), kPa	−216.5	−206.8	−201.8	−199.3	−189.9	−181.5	−179.5

Table 6. Stresses in slab with thickness of 260 mm.

TDA, %	0	10	20	40	60	80	100
Corner Loading							
Max stress, kPa	1182.2	1119.3	1082.2	1064.4	988.8	905.4	881.3
Max comp. stress (x-direction), kPa	936.3	894.1	884.5	878.3	846.2	801.5	787.0
Max tensile stress (x-direction), kPa	−108.4	−77.4	−60.7	−51.5	−15.2	0.0	0.0
Max comp. stress (y-direction), kPa	838.2	800.3	776.7	762.7	700.1	627.2	609.6
Max tensile stress (y-direction), kPa	−493.0	−458.2	−439.4	−429.1	−388.8	−349.6	−339.1
Interior Loading							
Max stress, kPa	−900.3	−845.8	−819.5	−805.6	−752.9	−702.3	−688.6
Max comp. stress (x-direction), kPa	118.0	127.7	132.9	135	138.1	133.9	131.6
Max tensile stress (x-direction), kPa	−900.3	−845.79	−819.5	−805.6	−752.9	−702.3	−688.6
Max comp. stress (y-direction), kPa	186.9	182.8	182.4	182	179.1	174.4	172.7
Max tensile stress (y-direction), kPa	−241.9	−238.2	−236.1	−235	−230.4	−225.7	−224.4
Edge Loading							
Max stress, kPa	−1664.2	−1558.9	−1508.2	−1481.5	−1380.9	−1285.1	−1259.3
Max comp. stress (x-direction), kPa	217.7	229.8	240.2	244.3	250.5	242.6	238.2
Max tensile stress (x-direction), kPa	−1664.2	−1558.9	−1508.2	−1481.5	−1380.9	−1285.1	−1259.3
Max comp. stress (y-direction), kPa	328.1	312.6	302.7	296.7	270.0	238.8	231.7
Max tensile stress (y-direction), kPa	−188.8	−180.7	−176.5	−174.3	−166.0	−158.4	−156.6

Table 7. Stresses in slab with thickness of 280 mm.

TDA, %	**0**	**10**	**20**	**40**	**60**	**80**	**100**
			Corner Loading				
Max stress, kPa	1041.5	993.7	960.0	948.8	885.8	817.8	797.9
Max comp. stress (x-direction), kPa	825.7	785.2	771.0	766.9	744.7	712.0	701.0
Max tensile stress (x-direction), kPa	−105.1	−80.5	−66.8	−59.2	−28.6	0.0	0.0
Max comp. stress (y-direction), kPa	735.1	707.7	690.1	679.7	631.7	573.6	556.0
Max tensile stress (y-direction), kPa	−438.3	−410.5	−395.1	−386.6	−352.4	−318.4	−309.1
			Interior Loading				
Max stress, kPa	−800.1	−752.5	−729.4	−717.2	−671.4	−627.5	−615.6
Max comp. stress (x-direction), kPa	102.5	104.0	110.1	112.7	118.6	118.0	116.8
Max tensile stress (x-direction), kPa	−800.1	−752.5	−729.4	−717.2	−671.4	−627.5	−615.6
Max comp. stress (y-direction), kPa	164.3	157.8	157.7	157.5	155.9	152.6	151.5
Max tensile stress (y-direction), kPa	−210.0	−207.0	−205.3	−204.4	−200.7	−196.7	−195.6
			Edge Loading				
Max stress, kPa	−1481.4	−1388.9	−1344.3	−1320.9	−1233.1	−1149.5	−1127.0
Max comp. stress (x-direction), kPa	188.8	186.2	198.2	203.2	215.0	214.1	211.8
Max tensile stress (x-direction), kPa	−1481.4	−1388.9	−1344.3	−1320.9	−1233.1	−1149.5	−1127.0
Max comp. stress (y-direction), kPa	287.5	276.9	269.6	265.2	244.8	219.9	212.4
Max tensile stress (y-direction), kPa	−166.1	−159.3	−155.7	−153.9	−146.6	−139.8	−138.1

Table 8. Stresses in slab with thickness of 300 mm.

TDA, %	**0**	**10**	**20**	**40**	**60**	**80**	**100**
			Corner Loading				
Max stress, kPa	922.9	886.2	856.0	845.1	796.8	741.1	724.6
Max comp. stress (x-direction), kPa	731.9	701.8	682.7	674.0	658.7	634.8	626.6
Max tensile stress (x-direction), kPa	−100.2	−80.6	−69.4	−63.1	−37.3	−10.7	−3.4
Max comp. stress (y-direction), kPa	648.7	628.6	615.6	607.7	570.7	524.5	510.2
Max tensile stress (y-direction), kPa	−391.5	−369.3	−356.7	−349.7	−320.8	−291.3	−283.2
			Interior Loading				
Max stress, kPa	−716.9	−674.6	−654.1	−643.5	−603.0	−564.5	−554.1
Max comp. stress (x-direction), kPa	89.1	88.5	91.0	93.9	101.7	103.7	103.3
Max tensile stress (x-direction), kPa	−716.9	−674.6	−654.1	−643.5	−603.0	−564.5	−554.1
Max comp. stress (y-direction), kPa	145.2	140.1	137.4	137.4	136.6	134.5	133.7
Max tensile stress (y-direction), kPa	−184.0	−181.6	−180.2	−179.5	−176.3	−173.0	−172.0
			Edge Loading				
Max stress, kPa	−1329.2	−1246.8	−1207.2	−1186.6	−1108.8	−1035.3	−1015.5
Max comp. stress (x-direction), kPa	163.9	163.4	163.0	168.7	184.0	188.2	187.5
Max tensile stress (x-direction), kPa	−1329.2	−1246.8	−1207.2	−1186.6	−1108.8	−1035.3	−1015.5
Max comp. stress (y-direction), kPa	253.6	246.1	240.7	237.5	221.9	202.2	196.1
Max tensile stress (y-direction), kPa	−147.2	−141.6	−138.5	−136.9	−130.5	−124.5	−122.9

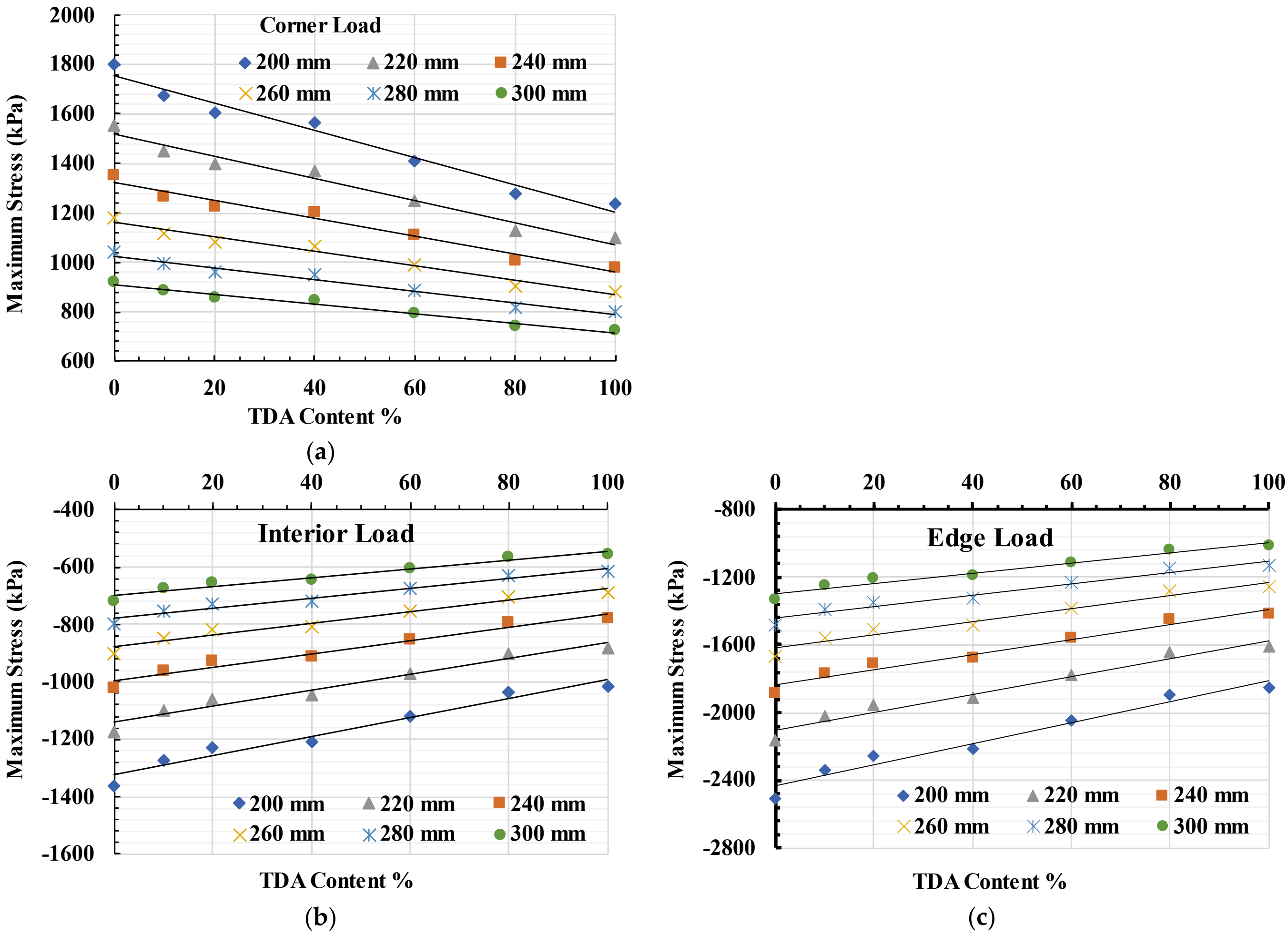

Figure 5. Variation of maximum stresses with slab thickness and TDA content. (**a**) corner loading, (**b**) interior loading, and (**c**) edge loading.

Figure 6 shows that vertical deflection increased with increasing TDA content. This is due to the decrease in the elastic modulus with a greater TDA content. For example, the deflection results for slabs with a thickness of 220 mm and different TDA contents can be compared in Figure 6. It shows that with the increase in TDA contents, the deflection increased under different loading conditions. For corner loading the increase in deflection ranged between 18% up to 94% for 10% and 100% TDA content, respectively. Other loading conditions yielded similar results with 18% up to 109% for 10% and 100% TDA content, respectively, for interior loading. As for edge loading, the increase ranged between 18% up to 101% for 10% and 100% TDA content, respectively. Results followed the same trend for all slab thicknesses and TDA content. This increased deflection may be attributable to the properties of the TDA, allowing PCC slabs containing TDA to deform more, and thus providing greater flexibility for rigid pavements under different loading conditions. Furthermore, results showed that with the increase in slab thicknesses the deflection decreased at the same TDA content. When comparing 220 mm slab with 0% TDA content and the 240 mm slab with 10% TDA content, as an example, both yielded approximately the same deflections under different loading condition. Although the increase in deflection seemed high for higher TDA contents, the absolute values for deflection from a design perspective did not increase significantly. For example, for the 220 mm slab, the deflection of a 0% TDA content was around 1.2 mm and 2.3 mm for 100% TDA.

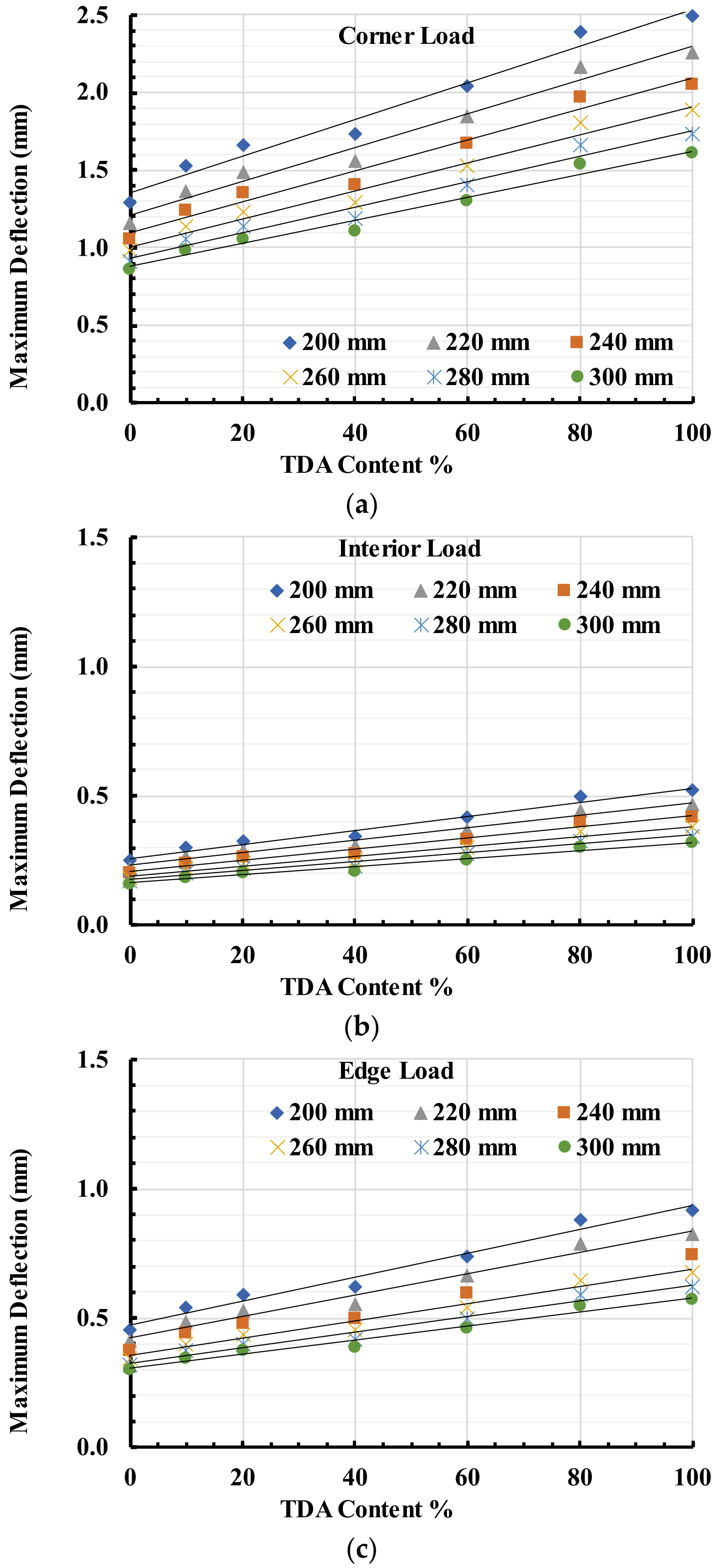

Figure 6. Variation of maximum deflection with slab thickness and TDA content. (**a**) corner loading, (**b**) interior loading, and (**c**) edge loading.

As shown in Table 9, damage analysis results varied significantly among mixes differing in slab thickness and TDA content. For instance, the cracking index of the slab with a thickness of 230 mm and 100% TDA indicated a drastic difference in the extent of damage. Increasing the slab thickness by 10 mm resulted in improved fatigue life, with a greatly reduced cracking index. For PCC mixes with 0, 10, and 20% TDA, *CI* values were 0 in thicker slabs, indicating that no failure would result from the applied load. For mixes with other TDA contents, there was a dramatic decrease in the *CI* values with the increase in slab thickness. Since KENPAVE utilizes the modulus of rupture to determine *CI*, and since the modulus of rupture decreased as the TDA content increased resulting in higher *CI*, however, it is postulated that due to the flexibility of TDA and its random distribution within the PCC mixes, TDA could act as a crack propagation inhibitor by absorbing stresses and flexing before failing, resulting in decreased fatigue failure due to loading, compared to mixes without TDA [20]. Li et al. [28] determined that when rubber was added to PCC mixes, the resulting impact energy was 2.39 times higher than in PCC mixes with no rubber, and the energy absorption capacity was increased by 9.46%.

Table 9. Cracking indices of the PCC slabs.

TDA, %	**0**	**10**	**20**	**40**	**60**	**80**	**100**
PCC Slab Thickness, mm				**Cracking Index (*CI*)**			
200	1.21×10^{-5}	2.60×10^{-4}	2.16×10^{-4}	4.09×10^{-3}	4.02×10^{-1}	3.80×10^{-1}	4.58×10^{0}
210	3.45×10^{-6}	6.68×10^{-5}	5.69×10^{-5}	8.77×10^{-4}	6.42×10^{-2}	6.30×10^{-2}	6.46×10^{-1}
220	6.39×10^{-7}	2.00×10^{-5}	1.73×10^{-5}	2.22×10^{-4}	1.24×10^{-2}	1.26×10^{-2}	1.12×10^{-1}
230	3.13×10^{-8}	6.77×10^{-6}	5.90×10^{-6}	6.52×10^{-5}	2.86×10^{-3}	2.97×10^{-3}	2.31×10^{-2}
240	0	1.99×10^{-6}	1.66×10^{-6}	2.16×10^{-5}	7.59×10^{-4}	8.05×10^{-4}	5.56×10^{-3}
250	0	3.59×10^{-7}	2.69×10^{-7}	7.97×10^{-6}	2.29×10^{-4}	2.47×10^{-4}	1.53×10^{-3}
260	0	0	0	2.77×10^{-6}	7.73×10^{-5}	8.42×10^{-5}	4.73×10^{-4}
270	0	0	0	6.86×10^{-7}	2.87×10^{-5}	3.16×10^{-5}	1.62×10^{-4}
280	0	0	0	7.86×10^{-8}	1.17×10^{-5}	1.29×10^{-5}	6.08×10^{-5}
290	0	0	0	0	4.91×10^{-6}	5.54×10^{-6}	2.47×10^{-5}
300	0	0	0	0	1.75×10^{-6}	2.08×10^{-6}	1.08×10^{-5}

4.3. Environmental Impacts and Cost Analyses

Energy consumption and emission results obtained for selected PCC slabs via the PaLATE 2.0 software are shown in Table 10. The results indicate an increase in environmental impacts with increased PCC slab thickness, and an overall decrease in environmental impacts with increased TDA content. The increase in TDA content was associated with a reduction in energy consumption ranging from 24,208 to 242,081 MJ (0.37% to 3.73%), a reduction in CO_2 emissions ranging from 1000 to 2000 kg (0.25% to 2.45%), and a reduction in NO_x emissions ranging from 18 to 177 kg (0.35% to 3.5%). The greatest improvements were a decrease in human toxicity potential (noncancer) ranging from 4.95% to 49.48%, and a decrease in human toxicity potential (cancer) ranging from 2.21% to 22.08%. However, it was found that with increased TDA content, SO_2 emissions increased slightly, by 0.05% to 0.46%. This can be attributed to the TDA treatment process. However, when environmental impacts due to disposing of rubber tires in landfill or incinerating them are taken into account, it can be seen that, overall, the use of TDA can be beneficial to the environment, especially if the results are applied to a full-scale rigid pavement project.

Table 10. Environmental impact results for selected PCC slabs.

Slab, mm	TDA	Energy (MJ)	Water Consumption (kg)	CO_2 (Mg) = GWP	NO_x (kg)	PM_{10} (kg)	SO_2 (kg)	CO (kg)	Hg (g)	Pb (g)	RCRA Hazardous Waste Generated (kg)	Human Toxicity Potential (Cancer) (kg)	Human Toxicity Potential (Noncancer) (kg)
200	0	5,191,814	2065	369	4048	1131	2910	1542	5.39	380	12,038	79,530	431,524,959
200	10%	5,172,448	2062	368	4034	1111	2911	1539	5.39	380	11,994	77,773	410,172,953
200	20%	5,153,081	2059	367	4020	1090	2912	1536	5.39	379	11,950	76,017	388,820,947
200	40%	5,114,348	2053	365	3992	1049	2915	1531	5.38	379	11,862	72,504	346,116,935
200	60%	5,075,615	2047	363	3963	1008	2918	1526	5.38	378	11,774	68,992	303,412,923
200	80%	5,036,882	2041	362	3935	967	2920	1521	5.37	377	11,686	65,479	260,708,910
200	100%	4,998,150	2035	360	3907	926	2923	1516	5.37	376	11,597	61,966	218,004,898
220	0	5,711,108	2272	406	4453	1244	3201	1696	5.93	418	13,242	87,486	474,683,196
220	10%	5,689,805	2269	405	4438	1222	3202	1693	5.93	418	13,194	85,554	451,195,989
220	20%	5,668,501	2265	404	4422	1199	3204	1690	5.93	417	13,145	83,622	427,708,783
220	40%	5,625,895	2259	402	4391	1154	3207	1684	5.92	416	13,048	79,758	380,734,369
220	60%	5,583,289	2252	400	4360	1109	3209	1679	5.92	416	12,951	75,894	333,759,956
220	80%	5,540,683	2246	398	4329	1064	3212	1673	5.91	415	12,854	72,030	286,785,542
220	100%	5,498,077	2239	396	4297	1019	3215	1667	5.91	414	12,757	68,166	239,811,129
240	0	6,230,401	2479	443	4858	1358	3492	1850	6.47	456	14,446	95,442	517,841,433
240	10%	6,207,161	2475	442	4841	1333	3493	1847	6.47	456	14,393	93,334	492,219,025
240	20%	6,183,922	2471	441	4824	1308	3495	1844	6.47	455	14,341	91,227	466,596,618
240	40%	6,137,442	2464	438	4790	1259	3498	1838	6.46	454	14,235	87,011	415,351,803
240	60%	6,090,963	2457	436	4756	1210	3501	1831	6.45	453	14,129	82,796	364,106,989
240	80%	6,044,483	2450	434	4722	1161	3505	1825	6.45	452	14,023	78,581	312,862,174
240	100%	5,998,004	2443	432	4688	1112	3508	1819	6.44	452	13,917	74,366	261,617,616
260	0	6,749,695	2685	480	5263	1471	3783	2004	7.01	494	15,650	103,398	560,999,669
260	10%	6,724,518	2681	478	5245	1444	3784	2001	7.01	494	15,593	101,115	533,242,062
260	20%	6,699,342	2677	477	5226	1418	3786	1998	7.00	493	15,536	98,831	505,484,454
260	40%	6,648,989	2670	475	5190	1364	3790	1991	7.00	492	15,421	94,265	449,969,238
260	60%	6,598,636	2662	473	5153	1311	3793	1984	6.99	491	15,307	89,698	394,454,022
260	80%	6,548,284	2654	470	5116	1258	3797	1977	6.99	490	15,192	85,132	338,938,806
260	100%	6,497,931	2646	468	5079	1204	3800	1971	6.98	489	15,077	80,565	283,423,590

Table 10. *Cont.*

Slab, mm	TDA	Energy (MJ)	Water Consumption (kg)	CO_2 (Mg) = GWP	NO_x (kg)	PM_{10} (kg)	SO_2 (kg)	CO (kg)	Hg (g)	Pb (g)	RCRA Hazardous Waste Generated (kg)	Human Toxicity Potential (Cancer) (kg)	Human Toxicity Potential (Noncancer) (kg)
280	0	7,268,988	2892	517	5668	1584	4074	2159	7.55	532	16,854	111,354	604,157,906
280	10%	7,241,875	2888	515	5648	1555	4076	2155	7.55	532	16,793	108,895	574,265,098
280	20%	7,214,762	2883	514	5629	1527	4077	2151	7.54	531	16,731	106,436	544,372,289
280	40%	7,160,536	2875	511	5589	1469	4081	2144	7.54	530	16,608	101,518	484,586,672
280	60%	7,106,310	2867	509	5549	1412	4085	2137	7.53	529	16,484	96,601	424,801,055
280	80%	7,052,084	2858	506	5509	1354	4089	2130	7.52	528	16,361	91,683	365,015,438
280	100%	6,997,858	2850	504	5470	1297	4093	2122	7.52	527	16,237	86,765	305,229,821
300	0	7,788,282	3098	553	6073	1697	4365	2313	8.09	570	18,058	119,310	647,316,143
300	10%	7,759,232	3094	552	6052	1666	4367	2309	8.09	570	17,992	116,675	615,288,134
300	20%	7,730,182	3089	551	6031	1636	4369	2305	8.08	569	17,926	114,041	583,260,125
300	40%	7,672,083	3080	548	5988	1574	4373	2297	8.08	568	17,794	108,772	519,204,107
300	60%	7,613,984	3071	545	5946	1513	4377	2290	8.07	567	17,662	103,503	455,148,088
300	80%	7,555,884	3062	543	5903	1451	4381	2282	8.06	566	17,529	98,234	391,092,070

As expected, cost analyses showed an increase in material costs with increased PCC slab thickness, due to the increased slab volume and amount of material required. In comparison to a 220 mm thick PCC slab, costs were 9.1% higher for a slab 240 mm thick and 18.2% higher for a slab 260 mm thick. In contrast, as shown in Figure 7, increased TDA content was associated with a 10% decrease in total material costs. This is attributable to the fact that the TDA replaces some of the natural coarse aggregates. Interestingly, it was found that the material costs of thicker slabs with 40% TDA were similar to those of thinner slabs with no TDA.

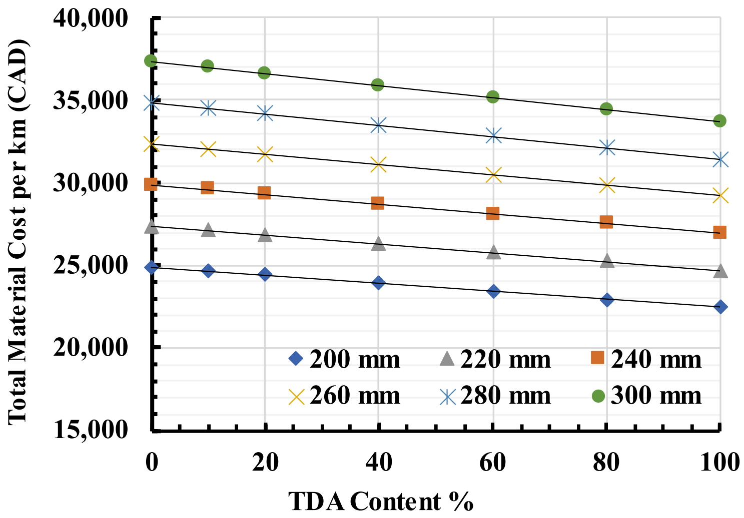

Figure 7. Costs analysis results.

5. Conclusions

In conclusion, this study shows that incorporating TDA in rigid pavement construction reduces environmental impacts and overall project costs by reducing the amount of natural material required. Although the use of TDA may reduce the cracking resistance of rigid pavements, the benefits cannot be ignored. In addition, the use of TDA improves the flexibility of PCC mixes, which can help to increase the tolerance to different loading conditions and reduce the failure potential. Thus, as demonstrated in this research, the use of TDA in rigid pavement construction as a replacement for natural coarse aggregates can achieve ecofriendly, sustainable rigid pavement design solutions.

The main findings of this study can be summarized as follows:

1. The strength and stiffness of the concrete decreased as the TDA content increased.
2. Increasing the concrete slab thickness reduced the stresses generated by various loading conditions. Increasing the TDA content similarly resulted in reduced stresses in the concrete slab.
3. Concrete slabs containing TDA exhibited greater flexibility and ductility than mixes without TDA. The ductility increased as the TDA content of the concrete increased, resulting in greater deflection in comparison to slabs without TDA.
4. PCC mixes with no TDA showed better cracking resistance in flexure than PCC mixes with TDA. For example, a PCC mix with no TDA exhibited a cracking resistance similar to that of a slab 10 mm thicker with 20% TDA.
5. An environmental impact analysis showed that incorporating TDA in PCC mixes reduced energy consumption and harmful emissions during material processing, transportation, and construction.
6. Cost analyses indicated increased material cost savings in PCC mixes with greater TDA content. For instance, a PCC slab with no TDA had material costs similar to those of a slab 10 mm thicker with 40% TDA.

Author Contributions: Conceptualization, A.M.A.A. and H.E.N.; methodology, A.M.A.A. and H.E.N.; software, A.M.A.A. and H.E.N.; validation, A.M.A.A. and H.E.N.; formal analysis, A.M.A.A. and H.E.N.; investigation, A.M.A.A. and H.E.N.; resources, A.M.A.A. and H.E.N.; data curation, A.M.A.A. and H.E.N.; writing—original draft preparation, A.M.A.A. and H.E.N.; writing—review and editing, A.M.A.A. and H.E.N.; visualization, A.M.A.A. and H.E.N.; supervision, A.M.A.A. and H.E.N.; project administration, A.M.A.A. and H.E.N.; funding acquisition, A.M.A.A. All authors have read and agreed to the published version of the manuscript.

Funding: This research was funded by Liwa College of Technology, Abu Dhabi, UAE, grant number IRG-ENG−001−2020.

Institutional Review Board Statement: Not applicable.

Informed Consent Statement: Not applicable.

Data Availability Statement: All produced data are presented in the paper.

Acknowledgments: The authors would like to express their gratitude to Liwa College of Technology, UAE, and Dalhousie University, Canada, for the provided support.

Conflicts of Interest: The authors declare no conflict of interest. The funders had no role in the design of the study; in the collection, analyses, or interpretation of data; in the writing of the manuscript, or in the decision to publish the results.

References

1. Saleh, H.M.; Eskander, S.B.; Fahmy, H.M. Mortar Composite Based on Wet Oxidative Degraded Cellulosic Spinney Waste Fibers. *Int. J. Environ. Sci. Technol.* **2014**, *11*, 1297–1304. [CrossRef]
2. Saleh, H.M.; Bondouk, I.I.; Salama, E.; Esawii, H.A. Consistency and Shielding Efficiency of Cement-Bitumen Composite for Use as Gamma-Radiation Shielding Material. *Prog. Nucl. Energy* **2021**, *137*, 103764. [CrossRef]
3. Robert, D.; Baez, E.; Setunge, S. A new technology of transforming recycled glass waste to construction components. *Constr. Build. Mater.* **2021**, *313*, 125539. [CrossRef]
4. Eskander, S.B.; Saleh, H.M.; Tawfik, M.E.; Bayoumi, T.A. Towards Potential Applications of Cement-Polymer Composites Based on Recycled Polystyrene FoamWastes on Construction Fields: Impact of Exposure toWater Ecologies. Case Stud. *Constr. Mater.* **2021**, *15*, e00664. [CrossRef]
5. Nasution, A.; Imran, I.; Abdullah, M. Improvement of Concrete Durability by Nanomaterials. *Procedia Eng.* **2015**, *125*, 608–612.
6. Saleh, H.M.; Bondouk, I.I.; Salama, E.; Mahmoud, H.H.; Omar, K.; Esawii, H.A. Asphaltene or Polyvinylchloride Waste Blended with Cement to Produce a Sustainable Material Used in Nuclear Safety. *Sustainability* **2022**, *14*, 3525. [CrossRef]
7. Abu Abdo, A.M.; Jung, S.J. Evaluation of Enforcing Rigid Pavements with Plastic Waste Fibers. *ARPN J. Eng. Appl. Sci.* **2019**, *14*, 2348–2355. Available online: http://www.arpnjournals.org/jeas/research_papers/rp_2019/jeas_0719_7814.pdf (accessed on 1 June 2022).
8. Eldin, N.N.; Senouci, A.B. Engineering properties of rubberized concrete. *Can. J. Civ. Eng.* **1992**, *19*, 912–923. [CrossRef]
9. Mills, B.; El Naggar, H.; Valsangkar, A. North American overview and Canadian perspective on the use of tire derived aggregate in highway embankment construction. In *Ground Improvement Case Histories*; Indraratna, B., Chu, J., Rujikiatkamjorn, C., Eds.; Elsevier Ltd.: Amsterdam, The Netherlands, 2015; Volume 2, pp. 635–655. [CrossRef]
10. Ashari, M.; El Naggar, H.; Martins, Y. Evaluation of the Physical Properties of TDA-Sand Mixtures. In Proceedings of the 70th Canadian Geotechnical Conference (GeoOttawa 2017), Ottawa, ON, Canada, 1–4 October 2017.
11. Bandarage, K.; Sadeghian, P. Effects of Long Shredded Rubber Particles Recycled from Waste Tires on Mechanical Properties of Concrete. *J. Sustain. Cem.-Based Mater.* **2020**, *9*, 50–59. [CrossRef]
12. El Naggar, H.; Soleimani, P.; Fakhroo, A. Strength and Stiffness Properties of Green Lightweight Fill Mixtures. *Geotech. Geol. Eng.* **2016**, *34*, 867–876. [CrossRef]
13. Mahgoub, A.; El Naggar, H. Using TDA underneath shallow foundations: Simplified design procedure. *Int. J. Geotech. Eng.* **2019**, *16*, 787–801. [CrossRef]
14. Mahgoub, A.; El Naggar, H. Using TDA as an Engineered Stress-Reduction Fill over Preexisting Buried Pipes. *J. Pipeline Syst. Eng. Pract.* **2019**, *10*, 4018034. [CrossRef]
15. Zahran, K.; Naggar, H. Effect of Sample Size on T.D.A. Shear Strength Parameters in Direct Shear Tests. *Transp. Res. Rec.* **2020**, *2674*, 1110–1119. [CrossRef]
16. Mahgoub, A.; El Naggar, H. Coupled TDA–Geocell Stress-Bridging System for Buried Corrugated Metal Pipes. *J. Geotech. Geoenviron. Eng.* **2020**, *146*, 4020052. [CrossRef]
17. Mahgoub, A.; El Naggar, H. Innovative Application of Tire-Derived Aggregate around Corrugated Steel Plate Culverts. *J. Pipeline Syst. Eng. Pract.* **2020**, *11*, 4020025. [CrossRef]
18. Mahgoub, A.; El Naggar, H. Shallow foundations on lightweight TDA backfill: Field tests and 3D numerical modelling. *Comput. Geotech.* **2020**, *126*, 103761. [CrossRef]

19. El Naggar, H.; Zahran, K.; Moussa, A. Effect of the Particle Size on the T.D.A. Shear Strength and Stiffness Parameters in Large-Scale Direct Shear Tests. *Geotechnics* **2021**, *1*, 1–17. [CrossRef]
20. El Naggar, H.; Zahran, K. Effect of the Particle Size on T.D.A. Shear Strength Parameters in Triaxial Tests. *Buildings* **2021**, *11*, 76. [CrossRef]
21. El Naggar, H.; Ashari, M.; Mahgoub, A. Development of an empirical hyperbolic material model for TDA utilizing large-scale triaxial testing. *Int. J. Geotech. Eng.* **2022**, *16*, 133–142. [CrossRef]
22. Taha, B.; Nounu, G. Utilizing Waste Recycled Glass as Sand/Cement Replacement in Concrete. *J. Mater. Civ. Eng.* **2009**, *21*, 709–721. [CrossRef]
23. Angelone, S.; Cauhapé Casaux, M.; Martinez, F.O. Green Pavements: Reuse of Plastic waste Fibers in Asphalt Mixtures. *Mater. Struct.* **2016**, *49*, 1655–1665. [CrossRef]
24. Hoppe, E.J.; Lane, D.S.; Fitch, G.M.; Shetty, S. Feasibility of Reclaimed Asphalt Pavement (RAP) Use as Road Base and Subbase Material. Virginia Center for Transportation Innovation and Research, Final Report VCTIR 15-R6, USA. 2015. Available online: https://www.virginiadot.org/vtrc/main/online_reports/pdf/15-r6.pdf (accessed on 1 June 2022).
25. Al-Tayeb, M.M.; Ismail, H.; Dawoud, O.; Wafi, S.R.; Daoor, I.A. Ultimate Failure Resistance of Concrete with Partial Replacements of Sand by Waste Plastic of Vehicles Under Impact Load. *Int. J. Sustain. Built Environ.* **2017**, *6*, 610–616. [CrossRef]
26. Abu Abdo, A.M.; Jung, S.J. Investigation of Reinforcing Flexible Pavements with Waste Plastic Fibers in Ras Al Khaimah, UAE. *Road Mater. Pavement Des.* **2020**, *21*, 1753–1762. [CrossRef]
27. Molenaar, A. Durability, A Prerequisite for Sustainable Pavements. In Proceedings of the 5th Eurasphalt and Eurobitume Congress, Istanbul, Turkey, 13–15 June 2012.
28. Li, H.; Xu, Y.; Chen, P.; Ge, J.; Wu, F. Impact Energy Consumption of High-Volume Rubber Concrete with Silica Fume. *Adv. Civ. Eng.* **2019**, *2019*, 1728762. [CrossRef]
29. Ghaly, A.M.; Cahill, J.D., IV. Correlation of Strength, Rubber Content, and Water to Cement Ratio in Rubberized Concrete. *Can. J. Civ. Eng.* **2004**, *32*, 1075–1081. [CrossRef]
30. Pham, T.M.; Elchalakani, M.; Hao, H.; Lai, J.; Ameduri, S.; Tran, T.M. Durability characteristics of lightweight rubberized concrete. *Constr. Build. Mater.* **2019**, *224*, 584–599. [CrossRef]
31. Huang, Y.H. *Pavement Analysis and Design*; Pearson Prentice Hall: Upper Saddle River, NJ, USA, 2004; pp. 147–236.
32. Coleman, L.W. Tire Recycling and the Environment: Benefits and Challenges. Hazardous and Solid Waste, Special Topics in Environmental Management. 22 March 2021. Available online: https://ehsdailyadvisor.blr.com/2021/03/tire-recycling-and-the-environment-benefits-and-challenges/ (accessed on 30 December 2021).
33. Dos Santos, J.; Thyagarajan, S.; Keijzer, E.; Flores, R.; Flintsch, G. Comparison of Life-Cycle Assessment Tools for Road Pavement Infrastructure. *Transp. Res. Rec.* **2017**, *2646*, 28–38. [CrossRef]
34. Horvath, A. A Life-Cycle Analysis Model and Decision-Support Tool for Selecting Recycled versus Virgin Materials for Highway Applications, Final Report for RMRC Research Project No. 23, University of California at Berkeley, USA. 2004. Available online: https://rmrc.wisc.edu/wp-content/uploads/2012/10/P23Final.pdf (accessed on 1 June 2022).
35. Bloom, E. Assessing the Life Cycle Benefits of Recycled Materials in Road Construction. Master's Thesis, University of Wisconsin, Madison, WI, USA, 2016. Available online: https://rmrc.wisc.edu/wp-content/uploads/2017/05/Bloom-Thesis_Final-Draft-V2.pdf (accessed on 1 June 2022).
36. Ganjian, E.; Khorami, M.; Maghsoudi, A.A. Scrap-tyre-rubber replacement for aggregate and filler in concrete. *Constr. Build. Mater.* **2009**, *23*, 1828–1836. [CrossRef]
37. Aslani, F. Mechanical properties of waste tire rubber concrete. *J. Mater. Civ. Eng.* **2016**, *28*, 14. [CrossRef]
38. Sparkes, J.; El Naggar, H.; Valsangkar, A. Compressibility and Shear Strength Properties of Tire-Derived Aggregate Mixed with Lightweight Aggregate. *J. Pipeline Syst. Eng. Pract.* **2019**, *10*, 4018031. [CrossRef]